Materials Research Proceedings 35 (2023) 198-205 https://doi.org/10.21741/9781644902714-24

Dimensional and geometric deviations of parts in PA12 manufactured by selective laser sintering: numerical and experimental analyses

Valentina Venditoli[1,a *], Achille Gazzerro[1,b], Wilma Polini[1,c] and Luca Sorrentino[1,d]

[1]Department of Civil and Mechanical Engineering, University of Cassino and Southern Lazio, via G. di Biasio 43, 03043 Cassino, Italy

[a]valentina.venditoli1@unicas.it, [b]achille.gazzerro@unicas.it, [c]polini@unicas.it, [d]sorrentino@unicas.it

Keywords: Additive Manufacturing, Inspection, Polymer

Abstract. Selective Laser Sintering (SLS) uses a laser to sinter powdered polymeric materials, such as Polyamide 12 (PA12). Industrially, it is commonly used as a mixture of virgin and aged powder. The aged powder has undergone various thermal cycles without being sintered. This work aims to evaluate the differences in the dimensional and geometrical deviations of parts in PA12 obtained through SLS by virgin and aged powder. A numerical approach was used to simulate the SLS software to foresee these dimensional deviations as a function of the powder's physical-chemical properties and the process parameters. The obtained results were validated through an experimental approach. Parallelepiped-shaped specimens were manufactured using an SLS printer and measured with a Coordinate Measuring Machine (CMM). The numerical results agree with the experimental ones. It seems that the differences between the dimensional deviations of the parts manufactured through virgin and aged powders are very small.

Introduction

In recent years, with the advent of Additive Manufacturing (AM), many technologies and materials have been implemented. These technologies favor the realization of layer-by-layer objects. Selective Laser Sintering (SLS) is an AM technique that uses the heat of a laser to sinter the portion of the material in a building chamber to obtain the required object layer-by-layer [1].

Most of the used materials are polymers [2]. Those plastic materials need low processing temperatures and laser power. The most commonly used material is Polyamide 12 (PA12). However, due to the printing process itself, since not all the powder is commonly sintered, 80% of it remains unused [3]; hence the material undergoes a thermal cycle, that changes its chemical and physical properties, leading to degradation effects affecting dimensional accuracy and mechanical performances [4, 5].

The printing process parameters, such as laser power, laser speed, scan spacing, and layer thickness, strongly influence the outcome, considering dimensional accuracy and mechanical performance. The energy density (ED) is defined as the energy concentrated in the area or in the volume of the part [6]; it takes into account the main printing parameters, and it is fundamental to achieve the required quality. A low ED provides weak sintering which means higher porosity and higher roughness. Moreover, the mechanical properties are lower. On the opposite side, using a high ED provides printed parts where the powder particles are bonded together, thus involving a low roughness and better mechanical properties. However, the dimensional accuracy is influenced by the higher shrinkage [7, 8]. Along the three-building direction, the x-direction maintains a higher dimensional accuracy regardless of the energy density. The accuracy along the y-direction deteriorates dramatically at high energy density levels. Finally, Z-direction accuracy was the lowest, with the highest values obtained at low energy densities. When energy density increased, accuracy steadily decreased [9].

Materials Research Proceedings 35 (2023) 198-205 https://doi.org/10.21741/9781644902714-24

When the effect of the laser power is analyzed, a drastic increase leads to a wide increase in shrinkage [10]. When comparing different layer thicknesses, the structural characteristics revealed obvious changes in the crystal structure of the polymer. Progressive crystal development with increasing layer thickness occurs in all construction orientations. In fact, dimensional accuracy and mechanical properties increase with smaller thicknesses [11].

However, it is also fundamental to recycle unsintered powder in the process in order to decrease manufacturing costs. This powder can be mixed in ratio with virgin one, to create a mixed powder, that can be reprocessed. Although being impacted by a variety of process factors, the dimensional accuracy of components printed with aged PA12 powders diminishes when compared to the initial item produced with virgin powder and the same settings [12]. Controlling the SLS process parameters, such as energy density and laser scanning approach, can help to minimize surface roughness and remove the "orange peel" effect [13].

According to different works, the change in mechanical performance is conflicting. This is most likely due to the numerous times the powder was utilized in these studies, the setting, and the used printer. Tensile strength improves somewhat throughout the first five buildings but drops by around 25% after the sixth build [14, 15].

This study intends to describe the dimensional deviations from the nominal of specimens printed in PA12 through the SLS process using PA12 virgin powder using both a numerical and an experimental approach. To accomplish this goal, ten parallelepiped-shaped specimens were designed, and once defined the values of the process parameters used to print, were manufactured numerically through simulation software. The obtained models of the manufactured parts were evaluated through inspection software to analyze the dimensional accuracy.

An experimental set-up was carried out to validate the numerical result. Further experimental tests were carried out using PA12 aged powder; the dimensional and geometrical deviations from nominal were measured through a coordinate measuring machine and the obtained results were compared with those due to the virgin powder.

The following is how the paper is organized: section 1 discusses the material properties, the printing machine, the used process parameters, and the numerical approach used to simulate the printing process. Section 2 presents the experimental setup and the measuring methods used to quantify specimen measurements. Section 3 presents the findings.

Material and methods

Following the ASTM D790-17 standard for flexural mechanical properties [16], parallelepiped-shaped specimens were designed, visible in Fig.1a, and all surfaces were nominated as shown in Fig.1b. Nylon 12 produced by Sintratec was used to manufacture the benchmarks and the main properties are shown in Table 1. Particularly, the set of specimens was manufactured using virgin powder and more than 5 times reused PA12 powder through the same values of the process parameters. The powder was subjected to consecutive printing processes without undergoing powder refreshing.

The numerical approach involves two steps: the simulation of the selective laser sintering process and that of the inspection process (see Fig.2). The SLS process was simulated through the Digimat® software package, Release 2022.1 [17] on which the reference input parameters on the type of the used printer and powder were imported.

In order to carry out a study able to significantly analyze the repeatability and potential of the simulation process, ten specimens were manufactured, five for two levels of the building volume (see Fig.3).

Inside the software, four steps were performed: definition, manufacturing, simulation, and outcomes analysis. The initial stage involves entering printer parameters, importing a benchmark, and specifying material.

Materials Research Proceedings 35 (2023) 198-205 https://doi.org/10.21741/9781644902714-24

For this purpose, the Sintratec-Kit printer was used [18], and it was equipped with a laser power of 2000 mW. The maximum buildable volume is 100 mm x 100 mm x 110 mm, while the maximum suggested volume is 90 mm x 90 mm x 90 mm. The machine is equipped with software that allows controlling the printing process. The parameters' set is constituted by a scan speed of 550 mm/s, a scan spacing of 0.1mm, and a layer height of 0.1mm. Furthermore, the chamber heating temperature was set at 140°C, the powder surface heating temperature at 150°C, and the melting temperature at 170 °C.

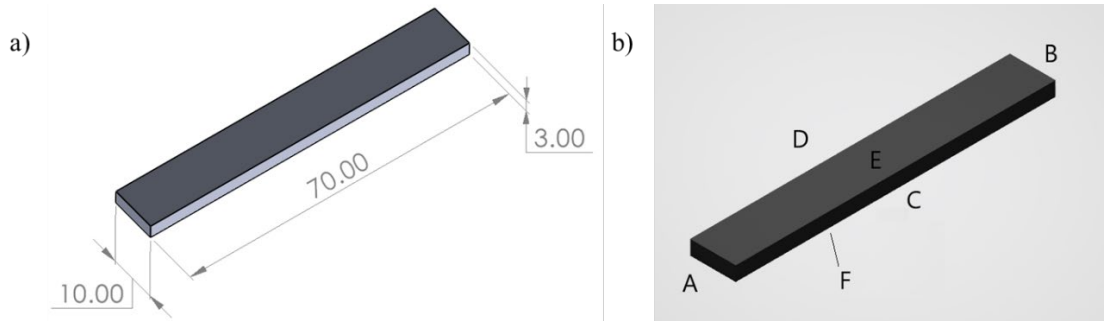

Fig. 1. (a) Benchmark dimensions in mm; (b) Surfaces.

Table 1. Nylon 12 thermo-physical properties.

Parameter	Value
Colour	Grey
Melting Point	176 °C, 348.8 F
Stable Temp (Max)	130 °C, 266 F
Bending Stress (Max)	43.1 MPa
Tensile Stress (Max)	47.8 MPa
Tensile Modulus (Max)	1750 MPa
Particle Size	0.06 mm (60 micron)

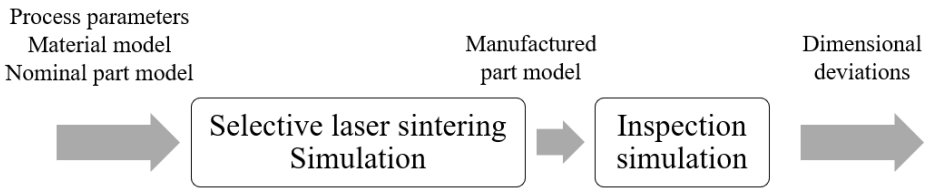

Fig. 2. Numerical approach.

For carrying out the simulation, the benchmark was discretized into a mesh voxel. The software recommended a voxel size between two and ten times the layer's height. For this work, a mesh size of 1 mm was used corresponding to the upper limit of the voxelization.

The output is saved as an STL file and loaded into the GOM Inspect software suite [19].

By analyzing the mesh, it was possible to compare the nominal CAD with the actual part to check the dimensional deviations. The step of the analysis consisted of creating reference elements through the Gaussian Best Fit method.

Materials Research Proceedings 35 (2023) 198-205 https://doi.org/10.21741/9781644902714-24

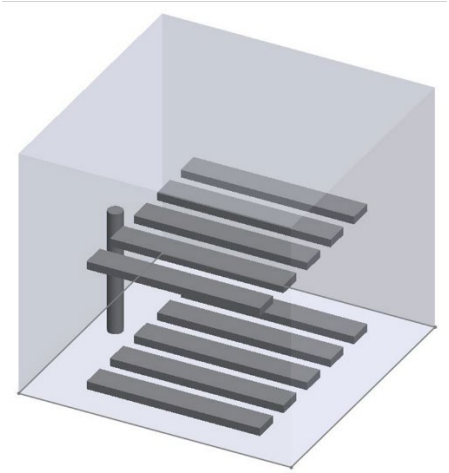

Fig. 3. Distribution of the specimens in the building chamber.

Experimental tests

Ten specimens placed on two levels were printed through the Sintratec-Kit printer as Fig.3, using the same process parameters of the numerical simulation.

The flexural specimens were measured using the coordinate measuring machine (CMM) of ZEISS. In order to perform this dimensional analysis, a type of fixture, visible in Fig.4a, b was chosen that does not geometrically deform the specimens.

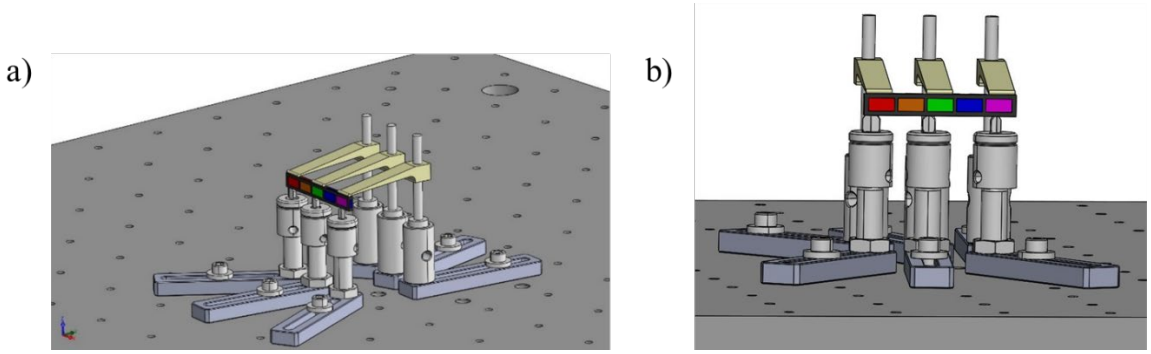

Fig. 4. (a, b) Benchmark's position on the CMM.

The Calypso software was used to analyse all the deviations presented in the specimens [20].

On the specimen, 5 areas were detected on the widest face, 2 on the side face, and 2 on the ends of the specimen. The coordinate measuring machine measured a set of points for each area; specifically on the broad face, 40 points were acquired for each area, while on the side and end areas, 8 points. From the measured points, the thickness, width, and length of the specimens were calculated. Finally, the averages were calculated since no significant difference was detected between the measured areas of each plane.

Result and discussion

The simulation result was superimposed on the reference geometry in the centerline to estimate any deviations in mm, that are shown in Fig.5. The deviations, presented in different colours, ranging from blue (smallest deviations) to red (largest deviations), are the dimensional changes of the part from the middle of the nominal geometry. By summing up the deviations on the endpoints, it will be possible to estimate the total deviation for each measurement.

Materials Research Proceedings 35 (2023) 198-205 https://doi.org/10.21741/9781644902714-24

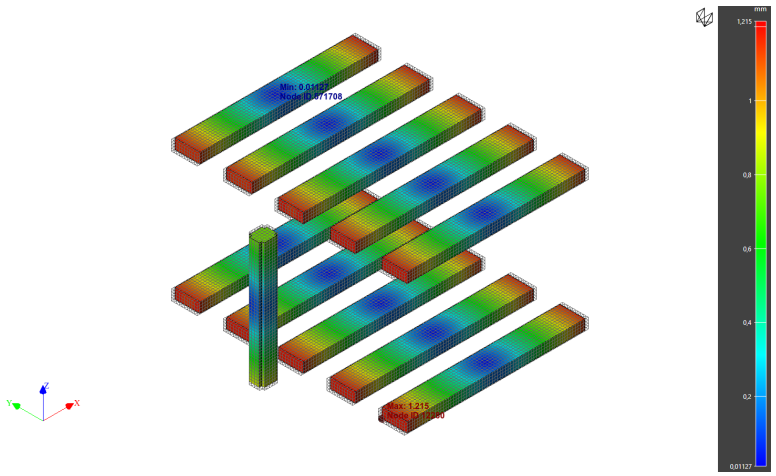

Fig. 5. Output from the numerical simulation.

For the ten specimens, the mean and standard deviation were calculated by the areas. From the results, it was observed that there was no significant difference among the different areas of the same plane for thickness, width, and length values. Therefore, all the data related to the different areas were put together. All the dimensions in the experimental, numerical, and nominal values were plotted in Fig.6.

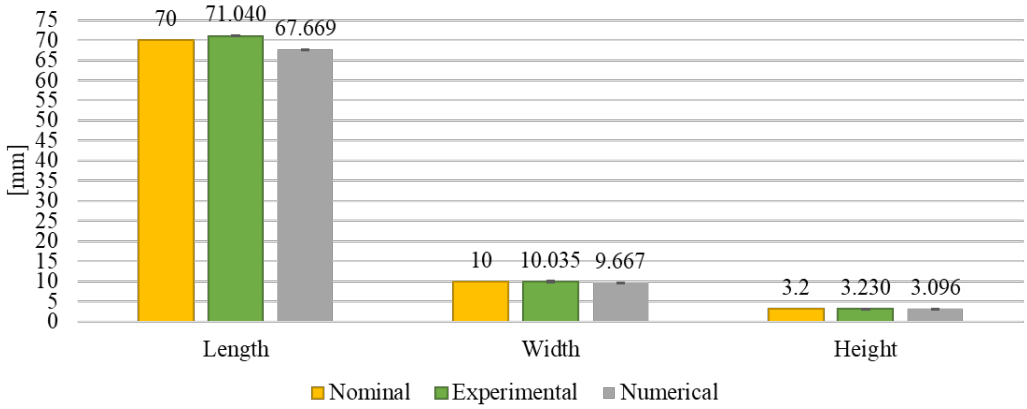

Fig. 6. Dimensional values using virgin PA12: comparison of experimental and numerical results.

From Fig.6 it can be seen that the experimental results are constantly bigger than the nominal ones. However, according to the specification of the printer, the obtained differences are inside the 5% accuracy declared by the printer builder.

Furthermore, the numerical results are smaller compared to the other results. This could be caused by the non-considered stress relaxation phenomena in the numerical simulation, so the shrinkage is higher [21, 22]. The percentage difference between the experimental and nominal results ranges from 0.35% to 1.49%, these values are inside the accuracy of the printer.

From 3% to 4% is the range of the percentage difference between experimental and numerical results, while the numerical results are smaller than the nominal ones of 3%, which is also confirmed in Fig.5.

The printing set-up (see Materials and methods) for the flexural specimens was repeated using aged PA12 powder, so further consideration can be given based on the used powder. A

Materials Research Proceedings 35 (2023) 198-205 https://doi.org/10.21741/9781644902714-24

comparison of the dimensional and geometrical deviations between virgin and recycled powder is listed in Fig.7 and Fig.8.

Fig.7 shows the average value of the dimensions of the ten specimens since there is no significant variation between specimens constructed on the bottom plane as well as those built on the top plane, as previously detected by manufacturing using virgin powder.

From the experimental results, there is no significant difference in the dimensional accuracy between the two manufacturing processes. Thus, the variance between virgin and n-times recycled powder is irrelevant, considering a variation in the difference of a maximum of 2%.

Further analysis where made, considering the geometric deviations of the specimens. In particular, the flatness of the planes of every specimen and the perpendicularity between the couples of planes were evaluated. At first, it was observed that there is no significant difference among the ten considered positions of the specimen on the printer volume. Therefore, the average for all ten positions was evaluated and reported in Fig.8.

It is possible to notice that the flatness values obtained experimentally range from 0.02 mm to 0.06 mm, while the perpendicularity values range from 0.04 mm to 0.07 mm.
It seems that in most measures there is no significant difference between virgin and recycled powder. It appears a large dispersion of the data, that increase of about 10% when the aged powder is used. However, there is some exception that requires further analysis.

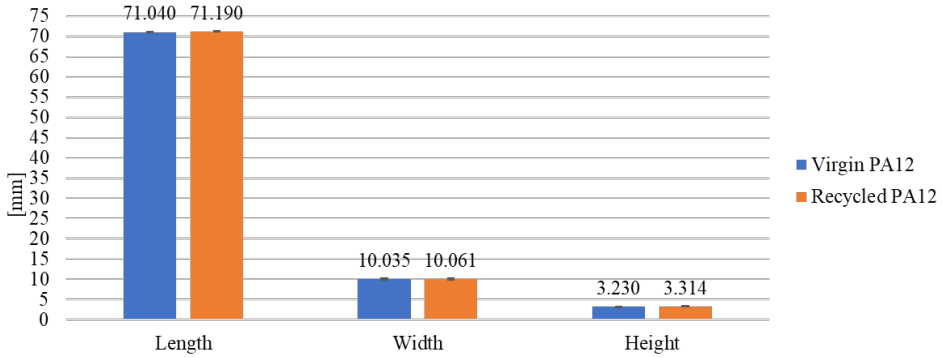

Fig. 7. Dimensional comparison between powders: experimental results.

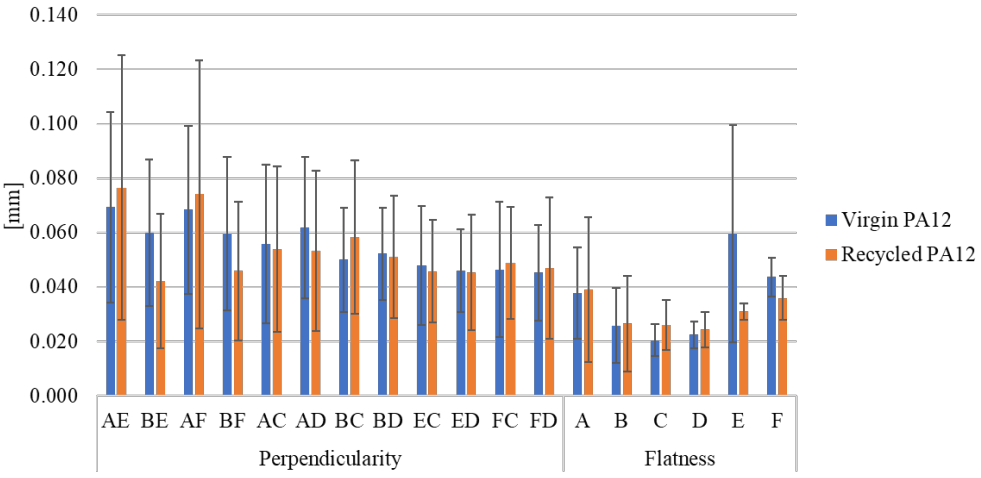

Fig. 8. Geometrical comparison between powders: experimental results.

Conclusion

The following work aimed to evaluate the dimensional deviations of components obtained through SLS with a 3D printer, making use of the Digimat® software.

Experimentally, ten flexural specimens made with the Sintratec Kit and the same process parameters as the simulated ones were manufactured. For such experimental data, a coordinate measuring machine was used to acquire multiple measurement points and extract the measurements of interest, and finally compare them with those obtained numerically.

The percentage variation between experimental and nominal results ranges from 0.35% to 1.49%, which is within the printer's declared accuracy of 5%.

The percentage difference between experimental and numerical findings ranges from 3% to 4%, whereas numerical results are 3% smaller than the nominal results. Additionally, the numerical findings are less than the other outcomes. This might be due to the numerical simulation failing to account for stress relaxation events, resulting in greater shrinkage.

Finally, the experimental procedure was repeated by changing the powder, and adopting a recycled PA12 of the same brand as the previous studies, and the obtained results were compared with those obtained previously.

The testing findings show that there is no statistically significant variation in dimensional accuracy between the two manufacturing procedures. Hence, with a maximum difference of 2%, the difference between virgin and n-times recycled powder is meaningless.

Further analyses were made on the geometric deviation connected with the parts manufactured. The experimentally achieved flatness values vary from 0.02 mm to 0.06 mm, whereas the perpendicularity values range from 0.04 mm to 0.07 mm.

Because the range in geometric outcomes is minor, geometric deviations are unaffected by the position in the construction chamber or the powder employed. In most cases, it appears that there is no discernible difference between virgin and recycled powder. However, there are several exceptions that demand an additional investigation.

Future studies should focus on the software characterization of aged powders, and residual stresses present within components in order to improve the reproducibility of parts made in SLS and investigate the mechanical performance to define the complete degradation. In addition, geometric deviations should be the subject of future studies to go to investigate future assemblies in objects of interest, experimentally and numerically.

Acknowledgments

This research did not receive any specific grant from funding agencies in the public, commercial, or not-for-profit sectors.

References

[1] S. Impey, P. Saxena, K. Salonitis, Selective Laser Sintering induced residual stresses: Precision measurement and prediction, Journal of Manufacturing and Materials Processing. 5 (2021) 101. https://doi.org/10.3390/jmmp5030101

[2] A. Awad, F. Fina, A. Goyanes, S. Gaisford, A.W. Basit, 3D printing: Principles and pharmaceutical applications of Selective Laser Sintering, International Journal of Pharmaceutics. 586 (2020) 119594. https://doi.org/10.1016/j.ijpharm.2020.119594

[3] L. Wang, A. Kiziltas, D.F. Mielewski, E.C. Lee, D.J. Gardner, Closed-loop recycling of polyamide12 powder from Selective Laser Sintering into sustainable composites, Journal of Cleaner Production. 195 (2018) 765–772. https://doi.org/10.1016/j.jclepro.2018.05.235

[4] K. Dotchev, W. Yusoff, Recycling of polyamide 12 based powders in the Laser Sintering Process, Rapid Prototyping Journal. 15 (2009) 192–203. https://doi.org/10.1108/13552540910960299

[5] D.T. Pham, K.D. Dotchev, W.A. Yusoff, Deterioration of polyamide powder properties in the Laser Sintering Process, Proceedings of the Institution of Mechanical Engineers, Part C: Journal of Mechanical Engineering Science. 222 (2008) 2163–2176. https://doi.org/10.1243/09544062jmes839

[6] A. Wegner, G. Witt, Correlation of process parameters and part properties in laser sintering using response surface modeling, Physics Procedia. 39 (2012) 480–490. https://doi.org/10.1016/j.phpro.2012.10.064
[7] E.C. Hofland, I. Baran, D.A. Wismeijer, Correlation of process parameters with mechanical properties of laser sintered PA12 parts, Advances in Materials Science and Engineering. 2017 (2017) 1–11. https://doi.org/10.1155/2017/4953173
[8] A. Wegner, C. Mielicki, T. Grimm, B. Gronhoff, G. Witt, J. Wortberg, Determination of robust material qualities and processing conditions for laser sintering of Polyamide 12, Polymer Engineering & Science. 54 (2013) 1540–1554. https://doi.org/10.1002/pen.23696
[9] T. Czelusniak, F.L. Amorim, Influence of energy density on polyamide 12 processed by SLS: From physical and mechanical properties to microstructural and crystallization evolution, Rapid Prototyping Journal. 27 (2021) 1189–1205. https://doi.org/10.1108/rpj-02-2020-0027
[10] J. Choren, V. Gervasi, T. Herman, S. Kamara, J. Mitchell, SLS powder life study, International Solid Freeform Fabrication Symposium. (2001).
[11] A. Liebrich, H.-C. Langowski, R. Schreiber, B.R. Pinzer, Effect of thickness and build orientation on the water vapor and oxygen permeation properties of laser-sintered polyamide 12 sheets, Rapid Prototyping Journal. 27 (2021) 1030–1040. https://doi.org/10.1108/rpj-05-2020-0101
[12] P. Chen, M. Tang, W. Zhu, L. Yang, S. Wen, C. Yan, et al., Systematical mechanism of polyamide-12 aging and its micro-structural evolution during Laser Sintering, Polymer Testing. 67 (2018) 370–379. https://doi.org/10.1016/j.polymertesting.2018.03.035
[13] W.A. Yusoff, The application of scanning electron microscope and melt flow index for Orange Peel in Laser Sintering process, Indonesian Journal of Electrical Engineering and Computer Science. 6 (2017) 615. https://doi.org/10.11591/ijeecs.v6.i3.pp615-622
[14] K. Kozlovsky, J. Schiltz, T. Kreider, M. Kumar, S. Schmid, Mechanical properties of reused nylon feedstock for powder-bed additive manufacturing in Orthopedics, Procedia Manufacturing. 26 (2018) 826–833. https://doi.org/10.1016/j.promfg.2018.07.103
[15] K. Wudy, D. Drummer, F. Kühnlein, M. Drexler, Influence of degradation behavior of polyamide 12 powders in laser sintering process on produced parts, AIP Conference Proceedings. (2014). https://doi.org/10.1063/1.4873873
[16] ASTM D 790, Plastics (I). Standard test methods for flexural properties of unreinforced and reinforced plastics and electrical insulating materials, Annual book of ASTM standards. American Society for Testing and Materials; 2017
[17] Digimat, Hexagon. https://www.mscsoftware.com/it/product/digimat (accessed February 22, 2023)
[18] Sintratec Kit. https://sintratec.com/product/sintratec-kit/ (accessed February 22, 2023)
[19] Gom Inspect software. https://www.gom.com/en/products/gom-suite/gom-inspect-pro (accessed February 22, 2023)
[20] Zeiss Calypso. https://www.zeiss.com/metrology/products/software/calypso-overview/calypso.html (accessed February 22, 2023)
[21] A. Al Rashid, M. Koç, Experimental validation of numerical model for thermomechanical performance of material extrusion additive manufacturing process: Effect of process parameters, Polymers. 14 (2022) 3482. https://doi.org/10.3390/polym14173482
[22] M.Q. Shaikh, P. Singh, K.H. Kate, M. Freese, S.V. Atre, Finite element-based simulation of metal fused filament fabrication process: Distortion Prediction and experimental verification, Journal of Materials Engineering and Performance. 30 (2021) 5135–5149. https://doi.org/10.1007/s11665-021-05733-0